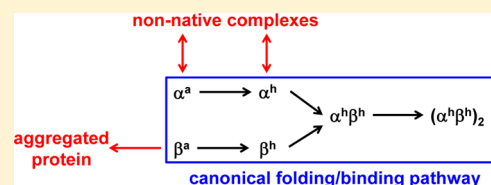


# Assembly of Hemoglobin from Denatured Monomeric Subunits: Heme Ligation Effects and Off-Pathway Intermediates Studied by Electrospray Mass Spectrometry

Jiangjiang Liu and Lars Konermann\*

Department of Chemistry, The University of Western Ontario, London, Ontario N6A 5B7, Canada

**ABSTRACT:** The oxygen binding properties of vertebrate hemoglobins (Hb) have been explored in great detail. In contrast, folding and assembly of these heterotetrameric protein complexes remain poorly understood. Similar to investigations of other multisubunit systems, *in vitro* Hb refolding experiments are often plagued by aggregation. Here we monitor the refolding of bovine Hb by electrospray mass spectrometry (ESI-MS). This technique allows the observation of coexisting subunit combinations, heme binding states, and protein conformers. Exposure to 40% acetonitrile at pH 10 causes Hb disassembly and extensive subunit unfolding. Hb reassembly is triggered by solvent exchange. Experiments conducted at room temperature provide a low metHb refolding yield. A significantly improved yield is achieved by lowering the temperature to 4 °C and by supplementing the protein solution with KCN prior to denaturation. Comparative studies under “low-yield” and “high-yield” conditions report on the interplay between folding and misfolding. The tendency of  $\beta$ -globin to undergo aggregation is found to be the key impediment to the formation of native Hb. The  $\alpha/\beta$  imbalance generated in this way favors the formation of non-native  $\alpha$ -globin assemblies. Our data imply that hemin dicyanide formed in the presence of KCN remains weakly bound to denatured  $\beta$ -globin, thereby counteracting aggregation, such that the refolding yield is enhanced. In the absence of aggregation-related interference, Hb assembly follows a symmetric pathway. Monomeric  $\alpha$ - and  $\beta$ -globin adopt a compact conformation upon heme binding. Heme-bound monomers then form heterodimers, and ultimately heterodimer association results in native Hb. This work highlights the utility of time-resolved ESI-MS investigations for interrogating the kinetic competition between on-pathway events and aberrant side reactions during the self-assembly of biomolecular complexes.



Considerable progress has been made in understanding the mechanisms by which small monomeric proteins fold to their native conformations.<sup>1</sup> The situation is more challenging for multisubunit systems. Protein complexes play a major role in numerous cellular processes.<sup>2</sup> Folding of these noncovalent assemblies requires the formation of intramolecular contacts, as well as intermolecular binding. In addition, many complexes incorporate metal ions or other cofactors.<sup>3–6</sup> Only relatively few time-resolved investigations of the folding and assembly of protein complexes have appeared in the literature.<sup>2,5</sup> Studies of this type are complicated by the fact that commonly used spectroscopic probes cannot readily distinguish between intra- and intermolecular events.<sup>7</sup> Also, the yield of folding–binding reactions tends to be low because of nonspecific aggregation.<sup>8,9</sup> On the other hand, similar aggregation phenomena can also occur *in vivo*. Thus, the observation of these off-pathway events *in vitro* can provide valuable insights into the kinetic competition between constructive binding and aberrant aggregation.<sup>8,10</sup>

Hemoglobin (Hb) acts as an oxygen transporter in red blood cells.<sup>11–13</sup> The native tetrameric Hb structure comprises two  $\alpha$  and two  $\beta$  subunits. The eight helices in  $\beta$ -globin are termed A–H. Helix D is missing in the slightly shorter  $\alpha$  subunit. The Hb quaternary structure represents an  $(\alpha^h \beta^h)_2$  dimer of dimers, where the superscript h indicates the presence of heme in each subunit. The tetramer is stabilized by hydrophobic contacts,

hydrogen bonds, van der Waals interactions, and salt bridges. The  $\alpha 1 \beta 1$  (and  $\alpha 2 \beta 2$ ) interfaces are linked by close contacts, whereas  $\alpha 1 \beta 2$  (and  $\alpha 2 \beta 1$ ) binding is less extensive.<sup>14</sup> Heme is sandwiched between helices E and F. Helix F provides the proximal ( $\alpha$ His87 and  $\beta$ His91) ligand for the heme iron. Reversible oxygen binding to ferrous ( $\text{Fe}^{2+}$ ) heme takes place on the distal side. Autoxidation can generate metHb (with ferric iron,  $\text{Fe}^{3+}$ ) that is incapable of  $\text{O}_2$  binding.<sup>15</sup>  $(\alpha^h \beta^h)_2$  can dissociate into  $\alpha^h \beta^h$ , with a tetramer–dimer  $K_d$  on the order of  $10^{-6}$  M for oxyHb.<sup>16,17</sup>

The oxygen binding properties of Hb have been explored in great detail.<sup>14,18</sup> In contrast, Hb folding and assembly are not as well understood. Hb can be refolded *in vitro* from isolated apoglobins ( $\alpha^a$  and  $\beta^a$ ) and free heme.<sup>19</sup> Deciphering the mechanism of this process is complicated by the substantial heterogeneity of the reaction mixture that comprises various subunit combinations and heme binding states.<sup>20,21</sup> Also, the refolding yield tends to be low because of the precipitation of  $\alpha^a$  and/or  $\beta^a$ .<sup>22</sup> Some earlier studies employed mixing of prefolded  $\alpha^h$  and  $\beta^h$ .<sup>23–26</sup> Assembly under these conditions requires the dissociation of non-native  $(\alpha^h)_2$  and  $(\beta^h)_4$  into monomeric species. This is followed by formation of  $\alpha^h \beta^h$ ,

**Received:** December 22, 2012

**Revised:** February 16, 2013

**Published:** February 18, 2013



which then generates  $(\alpha^h\beta^h)_2$ .<sup>21,26</sup> The extent to which other species such as  $\alpha^h\beta^a$  are involved as on-pathway or off-pathway intermediates remains unclear.<sup>20,24,27,28</sup> In red blood cell precursors, a chaperone termed AHSP ( $\alpha$ -hemoglobin-stabilizing protein) can sequester  $\alpha^h$  and/or  $\alpha^a$ , thereby suppressing aggregation and facilitating binding to  $\beta$ -globin.<sup>20,29</sup>

Native electrospray ionization (ESI) mass spectrometry (MS) reports on protein interactions and conformations. Via the transfer of intact noncovalent complexes into the gas phase, it is possible to determine their subunit stoichiometry via simple mass measurements.<sup>30–32</sup> Binding affinity estimates may be obtained from ion intensity ratios.<sup>33–35</sup> ESI charge state distributions are sensitive to the solution-phase conformation, because folded and unfolded proteins follow different ionization mechanisms.<sup>36</sup> Compact conformers form low charge states, whereas unfolded proteins generate wide distributions of highly protonated ions.<sup>37–41</sup> Thus, ESI-MS can simultaneously report on the assembly status and conformation of proteins.<sup>42</sup> Coexisting species can be monitored individually, whereas traditional spectroscopic tools provide only population-averaged data.<sup>39</sup> Via analysis of a reaction mixture at various time points, it is possible to uncover the temporal sequence of events during the assembly of noncovalent protein complexes.<sup>43–46</sup>

A number of studies have explored Hb subunit interactions by ESI-MS,<sup>28,34,45,47–50</sup> but a comprehensive view of the Hb folding–assembly mechanism is still lacking. The implications of recent unfolding studies<sup>28,50</sup> for the Hb refolding mechanism are not clear, because denaturation in those investigations was triggered by acidification, which induces irreversible heme precipitation.<sup>51</sup> Denaturants such as urea are problematic because they are incompatible with online ESI-MS. We recently monitored the refolding of metHb by ESI-MS, starting from monomeric subunits after acetonitrile-induced denaturation at basic pH.<sup>45</sup> In that work, it was possible to return the protein to a predominantly tetrameric state via solvent exchange.<sup>45</sup> Unfortunately, those earlier experiments<sup>45</sup> were conducted using Hb samples that had been obtained commercially as lyophilized powder. Subsequent investigations revealed that such commercial samples exhibit high levels of oxidative modifications that significantly affect the protein behavior and solubility.<sup>47,48,50</sup>

This work employs ESI-MS to investigate Hb refolding from denatured  $\alpha$ - and  $\beta$ -globin, using freshly prepared samples that are free of oxidative damage. Surprisingly, these high-quality samples exhibit a poor refolding yield when subjected to the refolding protocol of ref 45. Fortunately, a modified experimental approach that boosts the yield significantly can be developed. A side-by-side comparison of Hb refolding under “low-yield” and “high-yield” conditions offers the unique opportunity to uncover the mechanistic basis of the different outcomes. In this way, it is possible to obtain insights into the competition among folding, misfolding, aggregation, and the role of heme–protein interactions.

## EXPERIMENTAL PROCEDURES

**Materials.** Bovine oxyHb was purified as described from fresh cow blood that had been collected over 0.3% (w/v) sodium citrate.<sup>50</sup> Briefly, plasma and buffy coat were removed via centrifugation at 5500g for 30 min. The red blood cell pellet was washed with 0.9% (w/v) NaCl and recentrifuged four times. Red blood cells were ruptured osmotically by being exposed to distilled water with 10% (v/v) toluene. Stromal

impurities were extracted into the organic layer. The resulting hemolysate was centrifuged at 15000g for 30 min and dialyzed against 10 mM ammonium acetate with multiple buffer exchanges on ice. Stock solutions were flash-frozen in liquid nitrogen and stored at  $-80^\circ\text{C}$ . Mass analyses revealed that oxidative damage of Hb obtained in this way is negligible, consistent with earlier results.<sup>50</sup> Cyano-metHb was prepared by oxidizing oxyHb to metHb via addition of a 1.2-fold molar excess (on a heme basis) of potassium ferricyanide for 5 min at room temperature.  $\text{CN}^-$  binding was achieved by addition of a 1.2-fold molar excess of KCN. The resulting cyano-metHb was filtered through a 3 cm  $\times$  25 cm G-25 Sephadex column with 10 mM aqueous ammonium acetate (pH 7) as the mobile phase. The Hb subunit masses were found to agree with those expected on the basis of the amino acid sequence<sup>15</sup> (15053 Da for  $\alpha^a$  and 15954 Da for  $\beta^a$ ) to within  $\pm 1$  Da.

**Dialysis-Mediated Hb Refolding.** Denaturation of oxyHb was achieved by addition of ammonia to pH 10, followed by addition of 40% acetonitrile (v/v), for a final Hb concentration of 60  $\mu\text{M}$  (based on protein tetramers). Some experiments were conducted by adding 2 mM KCN to the protein solution prior to denaturation. After 7 min, 1 mL samples of denatured protein were transferred into a slide-A-Lyzer dialysis cassette (Pierce, Rockford, IL) with a 7 kDa molecular mass cutoff, followed by dialysis against 1 L of an aqueous ammonium acetate solution at pH 8. Solvent exchange reaches completion within 40 min.<sup>45</sup> Dialysis experiments were conducted at 22 or 4  $^\circ\text{C}$ . Aliquots were taken at various time points during dialysis for ESI-MS and for optical measurements. Control experiments with native Hb revealed a 27% decrease in protein concentration after dialysis for 18 h. Part of this effect is caused by the influx of the solution into the dialysis chamber, which leads to a 10% volume increase. The remainder (17%) is attributed to loss of the protein through the membrane.

**ESI Mass Spectrometry.** Hb samples were analyzed using a Q-TOF Ultima API instrument (Waters, Manchester, U.K.) equipped with a Z-spray source. Gentle ESI conditions that had previously been shown to preserve  $(\alpha^h\beta^h)_2$  complexes<sup>34</sup> were used (capillary voltage, 3 kV; cone voltage, 60 V; RF lens 1 voltage, 35 V; source temperature, 80  $^\circ\text{C}$ ; desolvation temperature, 40  $^\circ\text{C}$ ). Cone and desolvation gas flow rates were 150 and 500 L/h, respectively. The quadrupole profile was adjusted to ensure uniform transmission across the  $m/z$  range of interest.<sup>34</sup> The protein solution was infused into the ESI source at a rate of 5  $\mu\text{L}/\text{min}$  using a syringe pump. Each spectrum shown below represents the sum of 100 scans, with an acquisition time of 2 s per scan. All ESI-MS data were recorded at a nominal tetramer concentration of 60  $\mu\text{M}$ ; i.e., aliquots removed from the dialysis cassette were infused directly, without further processing or dilution. Signals in the ESI mass spectra were assigned via comparison of the measured peak positions with theoretical  $m/z$  values, calculated as  $m/z = (\text{total ion mass})/(\text{total ion charge})$ . For these calculations, it was noted that each protein ion signal corresponds to a linear combination of  $\alpha^a$  (15053 Da, charge of 0),  $\beta^a$  (15954 Da, charge of 0), heme (616.17 Da, charge of +1 due to oxidation during ESI),<sup>52</sup> proton (1.01 Da, charge of +1), potassium (39.1 Da, charge of +1), and cyanide (26.02 Da, charge of  $-1$ ).

**UV–Vis Spectroscopy.** Absorption spectra were recorded on a Varian (Palo Alto, CA) Cary 100 spectrophotometer. Data were acquired in 1 cm cuvettes. All samples were diluted to a nominal tetramer concentration of 2  $\mu\text{M}$ . Protein concentrations were determined using an  $\epsilon_{541}$  of 13.8  $\text{mM}^{-1}\text{cm}^{-1}$  for

oxyHb, of  $\epsilon_{500}$  of  $10.0 \text{ mM}^{-1} \text{ cm}^{-1}$  for metHb, and an  $\epsilon_{540}$  of  $11.5 \text{ mM}^{-1} \text{ cm}^{-1}$  for cyano-metHb.<sup>11,53</sup> These values are per heme equivalent; for determining the absorption coefficient of  $(\alpha^h\beta^h)_2$ , each value has to be multiplied by 4.

## RESULTS AND DISCUSSION

**Optical Studies of Hb Unfolding and Refolding.** Prior to ESI-MS investigations, it is instructive to characterize the protein behavior by UV-vis absorption spectroscopy. The heme absorption spectrum is sensitive to the porphyrin environment, iron ligation, and oxidation state. UV-vis measurements have been the primary tool for probing Hb structural changes for many years.<sup>11</sup>

Hb obtained using the isolation procedure outlined above displays a dominant Soret peak at 415 nm, along with maxima at 541 and 577 nm. The presence of these bands is consistent with oxyHb, where all ferrous heme groups are oxygenated (Figure 1A, black).<sup>11,50</sup> Hb denaturation was performed by exposure to 40% acetonitrile at pH 10.<sup>45</sup> The resulting spectrum has a greatly reduced Soret absorption with a maximum at 400 nm, reflecting major changes in the heme environment. At the same time, spectral alterations in the 500–600 nm range indicate the occurrence of heme  $\text{Fe}^{2+} \rightarrow \text{Fe}^{3+}$

autooxidation (Figure 1A, dashed red).<sup>11,15</sup> Hb denaturation conducted in the presence of 2 mM KCN results in a spectrum with a maximum at 426 nm (Figure 1A, blue), reflecting the formation of hemin-dicyanide  $\text{h}(\text{CN})_2$ .<sup>54,55</sup>

Hb refolding was triggered by dialysis-mediated acetonitrile removal, in combination with a decrease in pH from 10 to 8.<sup>45</sup> Initial experiments were conducted at 22 °C and in the absence of KCN. The UV-vis spectrum of Hb recorded 18 h after initiation of refolding displays a Soret maximum at 406 nm (Figure 1B, dashed red), consistent with metHb and distal ligation by  $\text{H}_2\text{O}$  or  $\text{OH}^-$ .<sup>11</sup> From the known metHb absorption coefficient (see Experimental Procedures), the refolding yield under these conditions can be determined to be ~48%. Partial aggregation and/or precipitation is the most likely culprit responsible for this low yield.<sup>22</sup> Interestingly, the same procedure results in a yield of almost 100% for commercially obtained metHb.<sup>45</sup> As noted in the introductory section, standard commercial samples are characterized by high oxidation levels at methionine and other residues, particularly for  $\beta$ -globin.<sup>50</sup> These oxidation events decrease the overall protein hydrophobicity<sup>56</sup> and thus reduce the aggregation propensity. Figure 1B reveals that the procedure of ref 45 performs poorly for the freshly prepared Hb used here, which is virtually free of oxidative modifications.

To improve the refolding conditions, the temperature was lowered to 4 °C, resulting in an increased yield of ~70% (data not shown). A further improvement to ~85% was achieved for Hb samples that had been supplemented with 2 mM KCN prior to denaturation. The UV-vis spectrum after refolding at 4 °C in the presence of KCN has a Soret maximum at 419 nm (Figure 1B, blue), corresponding to cyano-metHb where the distal coordination site is occupied by  $\text{CN}^-$ .<sup>11</sup> Similar experiments have previously been conducted with myoglobin.<sup>54,55</sup> The absorption properties of KCN-refolded Hb are virtually indistinguishable from those of freshly prepared cyano-metHb (Figure 1C). Control experiments conducted with KCl revealed that the enhanced refolding yield is not simply an ionic strength effect (data not shown).

Attempts to increase the refolding yield further via addition of free heme were not successful for any of the conditions employed here. This behavior indicates that the loss of free heme through the dialysis membrane is not a limiting factor, pointing to weak residual heme–protein interactions in the denatured state as suggested previously for other proteins such as myoglobin<sup>57</sup> and cytochrome  $b_{562}$ .<sup>58</sup>

In summary, the optical data of Figure 1 reveal that the Hb refolding behavior strongly depends on the conditions used. For investigating the mechanistic basis of the observed outcomes, we will focus on (i) low-yield conditions (22 °C without KCN) and (ii) high-yield conditions (4 °C with KCN). Free heme in the presence of KCN is converted to  $\text{h}(\text{CN})_2$  that is highly soluble and does not self-associate.<sup>54,55</sup> In the absence of KCN, heme has a much lower solubility, forming dimers and larger porphyrin aggregates at pH 8.<sup>51</sup>

**ESI-MS Characterization of Refolded Hb.** The UV-vis data of Figure 1 reflect only the local heme environment. Obtaining quaternary structural information requires the use of ESI-MS. For reference, Figure 2A shows a typical mass spectrum of native oxyHb. Monomeric subunits are virtually absent. The data are dominated by the canonical  $(\alpha^h\beta^h)_2$  assembly, with some contributions from  $\alpha^h\beta^h$ . For the instrument settings used here, the ion intensity ratio approximately matches the tetramer:dimer ratio in solution.<sup>34</sup>

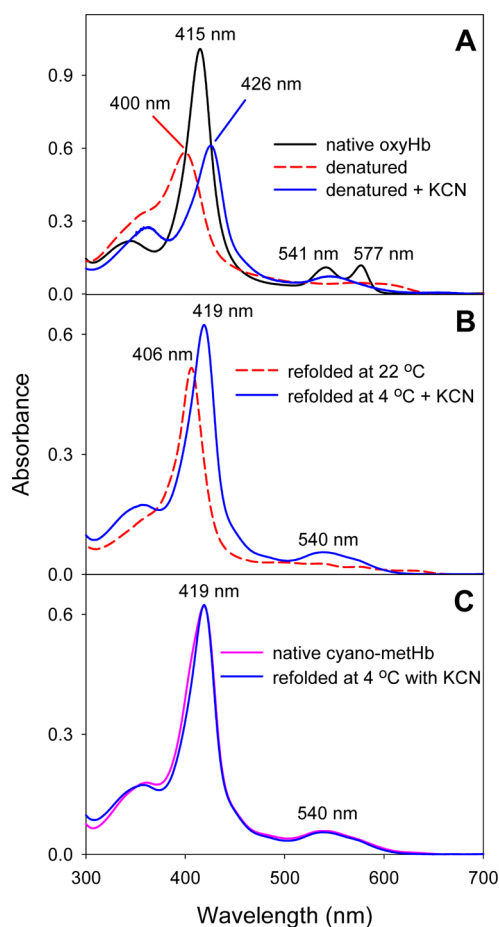


**Figure 1.** UV-vis absorption spectra of Hb under different conditions. (A) Freshly isolated oxyHb at pH 7 (black) and denatured Hb without KCN (red dashed) and with KCN (blue). (B) Hb after refolding at 22 °C without KCN (red dashed) and after refolding at 4 °C with KCN (blue). (C) Comparison of native cyano-metHb (pink) and Hb after refolding at 4 °C with KCN (blue).



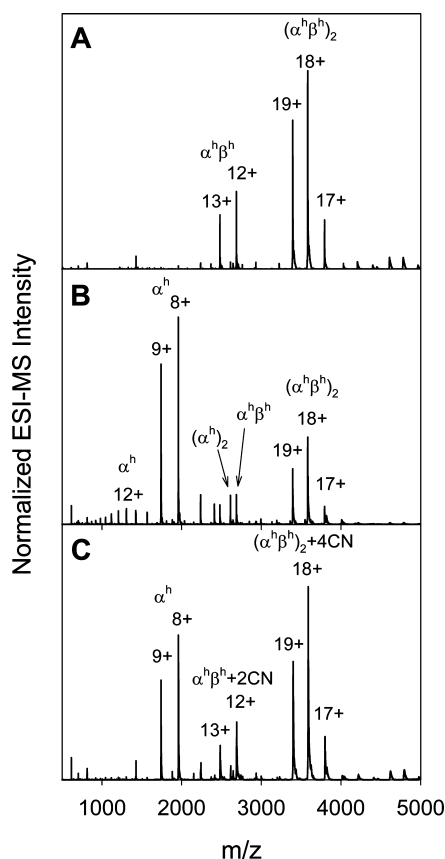


**Figure 2.** ESI mass spectra of (A) native oxyHb, (B) Hb after refolding under low-yield conditions (22 °C without KCN), and (C) Hb after refolding under high-yield conditions (4 °C with KCN). The protein ion notation is discussed in the text.

Quite a different spectrum is obtained after refolding under low-yield conditions (Figure 2B). The relative intensities of  $(\alpha^h\beta^h)_2$  and  $\alpha^h\beta^h$  are significantly reduced. Instead, the spectrum is dominated by  $\alpha^h$  in charge states +8 and +9, representing folded holo- $\alpha$ -globin monomers.<sup>39,45,50</sup> The spectrum also shows  $\alpha^h$  in higher charge states, originating from solution-phase conformers that are more unfolded. In addition, each  $\alpha^h\beta^h$  peak is accompanied by an  $(\alpha^h)_2$  satellite signal.

ESI-MS data obtained after high-yield refolding are dominated by cyanide-bound  $(\alpha^h\beta^h)_2$  (Figure 2C). The tetramer:dimer ratio resembles that of the native protein in Figure 2A. The contributions of free  $\alpha^h$  and  $(\alpha^h)_2$  in Figure 2C are significantly reduced relative to those in Figure 2B.

Overall, these ESI-MS data confirm that Hb samples after low-yield refolding are strongly perturbed (Figure 2B). In contrast, high-yield conditions mainly produce native tetramers (Figure 2C). Interestingly, the mass spectra of both refolded samples reveal an  $\alpha/\beta$  imbalance, where free  $\alpha^h$  and  $(\alpha^h)_2$  are not matched by any  $\beta$ -globin signals. Considering that the initial samples had an  $\alpha:\beta$  ratio of unity, this imbalance implies the loss of  $\beta$ -globin during refolding because of aggregation and/or precipitation. This  $\beta$ -globin deficiency is substantially more pronounced under low-yield conditions.

**Time-Dependent ESI-MS Measurements.** The Hb assembly status can be tracked during refolding by ESI-MS analysis of aliquots taken at various time points. Under low-yield conditions, the  $t = 0$  spectrum shows monomeric  $\alpha^a$ ,  $\alpha^h$ ,

$\beta^a$ , and  $\beta^h$  in a wide range of charge states (Figure 3A). These data confirm that the initial denaturing solvent environment

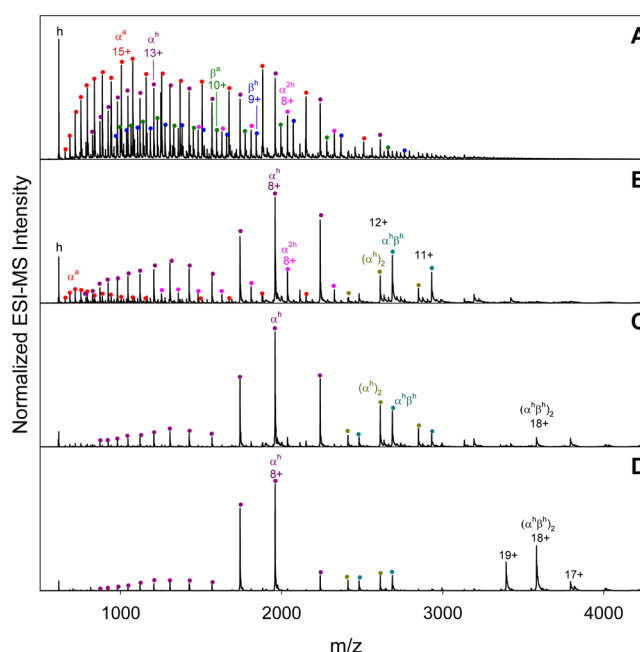


**Figure 3.** ESI-MS spectra taken at different time points during Hb refolding under low-yield conditions: (A) denatured state at 0 min (40% acetonitrile at pH 10), (B) 3 min, (C) 12 min, and (D) 18 h. Free heme is denoted as h.

produces a structurally heterogeneous ensemble of monomers.<sup>45</sup> The presence of apo and holo ions for both globins reveals that heme–protein interactions are not completely disrupted. The spectrum also shows  $\alpha$ -globin that is bound to a heme dimer ( $\alpha^h$ ) consistent with partial heme dimerization under the conditions used here.<sup>51</sup> Starting at  $t = 3$  min,  $\alpha^h$  ions in low charge states become the most abundant species (Figure 3B). In addition, there are notable contributions from  $\alpha^h\beta^h$  and  $(\alpha^h)_2$ . After 12 min,  $\alpha^a$  has all but vanished while  $(\alpha^h\beta^h)_2$  starts to appear (Figure 3C). Figure 3D represents the  $t = 18$  h end point of the reaction. Although the relative contribution of  $(\alpha^h\beta^h)_2$  has increased further, the spectrum remains dominated by  $\alpha^h$  in low charge states.

The data of Figure 3 provide interesting clues about why refolding at 22 °C without KCN results in a low  $(\alpha^h\beta^h)_2$  yield. Inspection of the mass spectra reveals that all time points show a  $\beta$ -globin deficiency. In particular, this imbalance is already apparent at time zero, where the combined signal intensities of  $\beta^a$  and  $\beta^h$  are roughly 3 times lower than those of  $\alpha^a$  and  $\alpha^h$  (Figure 3A). These observations point to aggregation-mediated loss of  $\beta$ -globin in the denatured state and early during refolding as the main reason underlying the low yield. Efforts to directly detect  $\beta$ -globin aggregates by scrutinizing the high mass range of the spectra were unsuccessful. Possible reasons for this behavior include mass heterogeneity and poor ionization efficiency.<sup>59</sup> An even more likely possibility is that aggregated  $\beta$ -globin adheres to the dialysis membrane. This view is supported by the fact that the absorption spectrum of the denatured protein in Figure 1A (dashed red) does not show an elevated Rayleigh scattering background in the short wavelength range, a phenomenon that would reveal the presence of aggregates in solution.<sup>60</sup>

ESI-MS data recorded under high-yield conditions provide a very different picture (Figure 4). Peak tailing results from

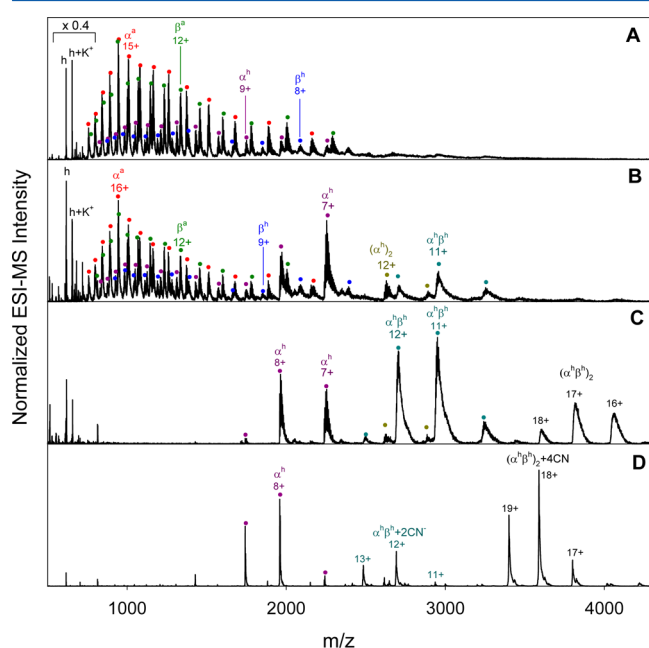


**Figure 4.** Refolding of Hb monitored by ESI-MS under high-yield conditions at (A) 0 min, (B) 3 min, (C) 12 min, and (D) 18 h. The intensity in the free heme region of panel A has been rescaled, as indicated.

adduct formation caused by the presence of KCN in the solution. Salt effects of this kind are well-known in ESI-MS.<sup>61</sup> For the spectra of Figure 4, the extent of adduct formation decreases as the salt concentration decreases during dialysis. The denatured state in the presence of KCN displays non-native charge state distributions for both globins (Figure 4A), similar to those seen under low-yield conditions (Figure 3A). Strikingly, however, Figure 4A shows comparable ion intensities for  $\alpha^a$  and  $\beta^a$ , as well as for  $\alpha^h$  and  $\beta^h$ . In other words, the  $\alpha/\beta$  imbalance at time zero is much less pronounced in the presence of KCN. Nonetheless, signs of  $\beta$ -globin deficiency start to appear after 3 min (Figure 4B). At this time point, a close match in  $\alpha$  and  $\beta$  intensities is seen only for highly charged ions. In contrast, the low-charge state range displays dominant  $\alpha^h$  signals, as well as  $(\alpha^h)_2$  without matching  $\beta$ -globin contributions.  $\alpha^h \beta^h$  dominates the spectrum after 12 min (Figure 4C). After 18 h, most of the  $\alpha^h \beta^h$  has assembled into native Hb tetramers (Figure 4D), but a significant contribution of monomeric  $\alpha^h$  remains. Thus, a deficiency of freely available  $\beta$ -globin limits the  $(\alpha^h \beta^h)_2$  assembly process even under the high-yield conditions of Figure 4, although the extent of this deficiency is much less pronounced than in the absence of KCN (Figure 3).

**Hb Assembly Mechanism.** Figure 5 summarizes the spectral changes accompanying the Hb assembly process under low-yield and high-yield conditions. Temporal ESI-MS intensity profiles were generated from the measured peak areas, integrated over all charge states for any given species.

Under both conditions,  $\alpha^a$  is consumed within a few minutes (Figure 5A,B). Under low-yield conditions, this  $\alpha^a$  disappearance is mirrored by accumulation of  $\alpha^h$ , caused by a shortage of suitable binding partners, i.e.,  $\beta$ -globin. This shortage is apparent from the low  $\beta^a$  and  $\beta^h$  intensities in Figure 5C.  $\alpha^h$

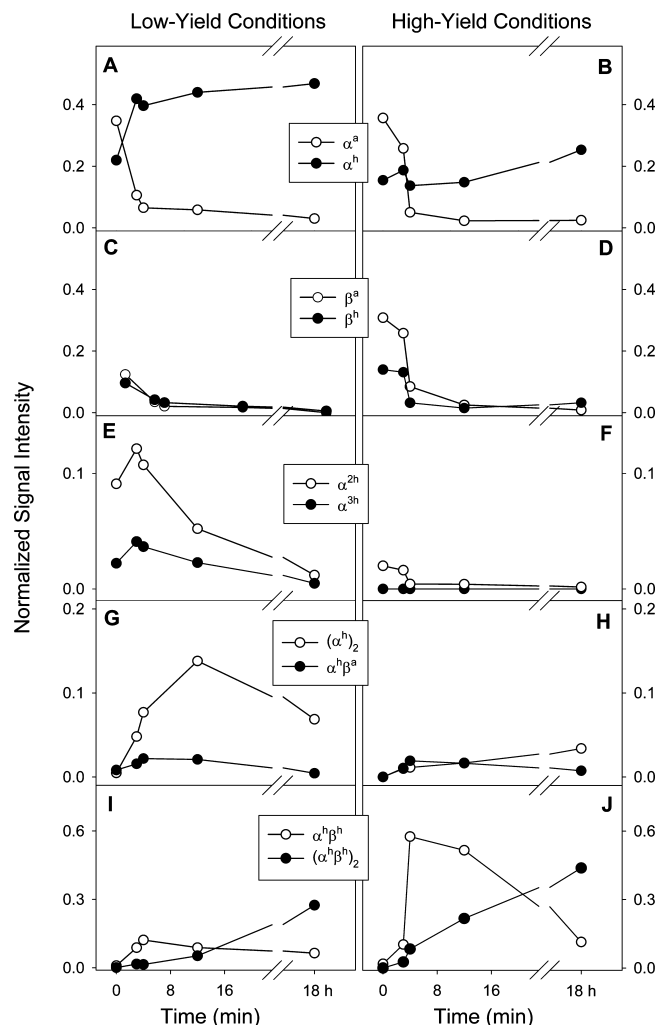


**Figure 5.** Refolding kinetics of Hb monitored by ESI-MS under low-yield conditions (left column) and under high-yield conditions (right column). These data correspond to signal intensities that were integrated over all charge states for each individual species. Note the differences in intensity axis scaling.

accumulation is less pronounced under high-yield conditions (Figure 5B) because of a more abundant supply of  $\beta$ -globin (Figure 5D). Low-yield conditions cause an initial buildup of  $\alpha^{2h}$  and  $\alpha^{3h}$ , followed by the complete disappearance of these species at later reaction times (Figure 5E). Thus, while  $\alpha^{2h}$  and  $\alpha^{3h}$  represent off-pathway intermediates, they ultimately equilibrate with other species and are consumed during the reaction. Neither  $\alpha^{2h}$  nor  $\alpha^{3h}$  becomes significantly populated under high-yield conditions (Figure 5F). This observation reflects the fact that heme retains a soluble monomeric state  $[\text{h}(\text{CN})_2]$  in the presence of KCN,<sup>54,55</sup> whereas partial heme aggregation takes place under low-yield conditions.<sup>51</sup> Heme dimer and trimer binding has previously been observed for myoglobin.<sup>62</sup>

$(\alpha^h)_2$  is another off-pathway intermediate that transiently accumulates under low-yield conditions (Figure 5G). In earlier work, this species has been detected in  $\beta$ -globin-free solutions.<sup>21,26</sup> Thus, it is not surprising that  $(\alpha^h)_2$  formation is suppressed in the presence of KCN (Figure 5H) where a larger supply of  $\beta$ -globin is available.

According to one proposed model, the formation of  $\alpha^h \beta^h$  generally proceeds via association of  $\alpha^h$  with  $\beta^a$ , followed by

heme binding. This scenario would involve  $\alpha^h\beta^a$  as an obligatory intermediate.<sup>27,28</sup> In an alternative mechanism,  $\alpha^h\beta^h$  is formed by binding of  $\alpha^h$  to  $\beta^h$ .<sup>45,50</sup> Our data confirm the presence of  $\alpha^h\beta^a$ , albeit with very low abundance [ $<2\%$  (Figure 5G,H)]. In comparison, the abundance of  $\alpha^h\beta^h$  reaches much higher values, i.e., 12% (Figure 5I) and 58% (Figure 5J). The absence of a lag phase between formation of  $\alpha^h\beta^h$  and  $\alpha^h\beta^a$  suggests that the latter is not an obligatory intermediate under the in vitro conditions of this work. Nonetheless, we cannot exclude the possibility that a subpopulation of  $\alpha^h\beta^h$  is formed via binding of heme to  $\alpha^h\beta^a$ .<sup>27,28</sup> Thus, our data are compatible with  $\alpha^h\beta^a$  as an optional intermediate during Hb assembly. However, formation of  $\alpha^h\beta^h$  as a result of binding of  $\alpha^h$  to  $\beta^h$  appears to be the dominant pathway. Regardless of these considerations, it is clear that formation of  $(\alpha^h\beta^h)_2$  from two  $\alpha^h\beta^h$  units represents the final step of the Hb assembly process (Figure 5I,J).<sup>21,26</sup>

**High-Yield versus Low-Yield Conditions.** We now return to the question of why refolding at 4 °C with KCN provides a higher yield than at 22 °C without KCN. Elevated temperatures generally enhance the Boltzmann population of partially disordered conformers that are prone to aggregation.<sup>63</sup> Thus, it is not surprising that 4 °C provides refolding conditions that are more favorable. The second factor responsible for enhancing the refolding yield in our experiments is the presence of KCN. As noted above,  $\text{CN}^-$  induces the formation of  $\text{h}(\text{CN})_2$  that is highly resistant to self-association.<sup>54,55</sup> The key problem that limits the refolding yield in our experiments is aggregation and/or precipitation of  $\beta$ -globin. Our data reveal that KCN helps to maintain  $\beta$ -globin in a soluble state. It is well-known that the stability of monomeric apoglobins depends on the presence of heme.<sup>20,64</sup> It is also known that heme is a promiscuous binding partner that can weakly interact with proteins even under denaturing conditions.<sup>57,58,65,66</sup> Considering this background information, we propose that residual  $\text{h}(\text{CN})_2$ –protein interactions act to stabilize  $\beta$ -globin, thus counteracting the tendency of the protein to precipitate and promoting its availability as a binding partner during Hb assembly. In other words, we propose that a significant fraction of the “apo”- $\beta$ -globin ions in Figure 4 are derived from denatured proteins that were engaged in weak residual interactions with  $\text{h}(\text{CN})_2$  in solution. The exact nature of these interactions cannot be determined by our experiments, but the interactions likely involve hydrophobic elements. The disruption of such weakly bound complexes during ESI is to be expected.<sup>67</sup>

## CONCLUSIONS

Studies of the folding and assembly of multiprotein complexes are often plagued by the occurrence of nonspecific aggregation phenomena that limit the overall yield.<sup>8,9</sup> This work offers a unique opportunity to explore the kinetic competition between successful self-assembly and aggregation-mediated protein loss. Comparative time-dependent ESI-MS measurements conducted under low-yield and high-yield conditions provide insights into the reasons underlying the different outcomes. Our findings can be summarized using a simple flowchart (Figure 6). In the absence of any interfering factors, semidenatured  $\alpha^a$  and  $\beta^a$  fold into compact  $\alpha^h$  and  $\beta^h$  conformers, respectively. The holo monomers bind to form  $\alpha^h\beta^h$ . Association of these heterodimers ultimately results in the native  $(\alpha^h\beta^h)_2$  state (black arrows). Aberrant side reactions are highlighted in red. Under high-yield conditions, these side

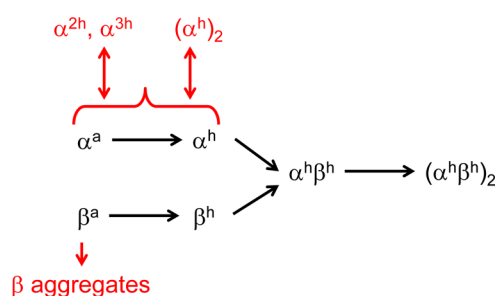


**Figure 6.** Cartoon depiction of the Hb assembly process. Unidirectional steps are represented by single-headed arrows. Double-headed arrows denote reversible events. The main folding–assembly pathway is colored black. Aberrant side reactions are colored red. Under high-yield conditions, these side reactions are suppressed.

reactions are suppressed. Loss of  $\beta$ -globin due to irreversible aggregation represents the main problem. Lowering the temperature helps to maintain this subunit in solution. In addition, residual heme–protein interactions appear to be crucial in preventing  $\beta$ -globin aggregation. The preservation of these interactions is promoted by KCN, because cyanide binding counteracts the tendency of heme to self-associate. The formation  $\alpha$ -globin off-pathway intermediates depends on the availability of  $\beta$ -globin. Dimerization of  $\alpha^h$  is favored if the  $\beta$ -globin supply is limited. In addition,  $\alpha$ -globin can bind to small heme aggregates, thus forming  $\alpha^{2h}$  and  $\alpha^{3h}$ . It is quite possible that sequestering heme in this way further promotes the precipitation-mediated loss of  $\beta$ -globin. In support of this idea, previous work has demonstrated that globin folding can be limited by slow heme dimer dissociation.<sup>68</sup>

Overall, this work demonstrates that time-dependent ESI-MS investigations provide detailed insights into the assembly mechanisms of protein complexes, the role of on- and off-pathway intermediates, and the kinetic competition between assembly and aggregation. In future studies, the incorporation of ion mobility measurements<sup>69</sup> and online hydrogen exchange<sup>62</sup> will be promising avenues for obtaining an even deeper understanding of biomolecular self-assembly.

## AUTHOR INFORMATION

### Corresponding Author

\*Telephone: (519) 661-2111, ext. 86313. Fax: (519) 661-3022. E-mail: konerman@uwo.ca.

### Funding

This work was supported by the Natural Sciences and Engineering Council of Canada and by the Canada Research Chairs Program.

### Notes

The authors declare no competing financial interest.

## ABBREVIATIONS

$\alpha^h$ , holo- $\alpha$ -globin;  $\alpha^a$ , apo- $\alpha$ -globin;  $\beta^h$ , holo- $\beta$ -globin;  $\beta^a$ , apo- $\beta$ -globin; AHSP,  $\alpha$ -hemoglobin-stabilizing protein; ESI, electrospray ionization;  $\text{h}(\text{CN})_2$ , hemin dicyanide; Hb, hemoglobin; MS, mass spectrometry; metHb, met-hemoglobin (heme iron in the +3 oxidation state).

## REFERENCES

- (1) Wolynes, P. G., Eaton, W. A., and Fersht, A. R. (2012) Chemical physics of protein folding. *Proc. Natl. Acad. Sci. U.S.A.* 109, 17770–17771.



- (2) Rumfeldt, J. A. O., Galvagnion, C., Vassall, K. A., and Meiering, E. M. (2008) Conformational stability and folding mechanisms of dimeric proteins. *Prog. Biophys. Mol. Biol.* 98, 61–84.
- (3) Boehr, D. D., Nussinov, R., and Wright, P. E. (2009) The role of dynamic conformational ensembles in biomolecular recognition. *Nat. Chem. Biol.* 5, 789–796.
- (4) Wittung-Stafshede, P. (2002) Role of Cofactors in Protein Folding. *Acc. Chem. Res.* 35, 201–208.
- (5) Kiefhaber, T., Bachmann, A., and Jensen, K. S. (2012) Dynamics and mechanisms of coupled protein folding and binding reactions. *Curr. Opin. Struct. Biol.* 22, 21–29.
- (6) Verkhrivker, G. M., Bouzida, D., Gehlhaar, D. K., Rejto, P. A., Freer, S. T., and Rose, P. W. (2003) Simulating disorder-order transition in molecular recognition of unstructured proteins: Where folding meets binding. *Proc. Natl. Acad. Sci. U.S.A.* 100, 5148–5153.
- (7) Bartlett, A. I., and Radford, S. E. (2009) An expanding arsenal of experimental methods yields an explosion of insights into protein folding mechanisms. *Nat. Struct. Mol. Biol.* 16, 582–588.
- (8) Pastore, A., and Temussi, P. A. (2012) The two faces of Janus: Functional interactions and protein aggregation. *Curr. Opin. Struct. Biol.* 22, 30–37.
- (9) Mishra, R., Seckler, R., and Bhat, R. (2005) Efficient refolding of aggregation-prone citrate synthase by polyol osmolytes: How well are protein folding and stability aspects coupled? *J. Biol. Chem.* 280, 15553–15560.
- (10) Seckler, R. (2000) Assembly of multi-subunit structures. In *Mechanisms of Protein Folding* (Pain, R. H., Ed.) 2nd ed., pp 279–308, Oxford University Press, Oxford, U.K.
- (11) Antonini, E., and Brunori, M. (1971) *Hemoglobin and Myoglobin in Their Reactions With Ligands*, Vol. 21, North-Holland Publishing Co., Amsterdam.
- (12) Dickerson, R. E., and Geis, I. (1983) *Hemoglobin: Structure, Function, Evolution, and Pathology*, The Benjamin/Cummings Publishing Co., Inc., Menlo Park, CA.
- (13) Bunn, H. F., and Forget, B. G. (1986) *Hemoglobin: Molecular, Genetic and Clinical Aspects*, W. B. Saunders Co., Philadelphia.
- (14) Perutz, M. F. (1970) Stereochemistry of Cooperative Effects in Haemoglobin. *Nature* 228, 726–739.
- (15) Aranda, R., IV, Cai, H., Worley, C. E., Levin, E. J., Li, R., Olson, J. S., Phillips, G. N., Jr., and Richard, M. P. (2009) Structural analysis of fish versus mammalian hemoglobins: Effect of the heme pocket environment on autooxidation and heme loss. *Proteins* 75, 217–230.
- (16) Riggs, A. F. (1998) Self-association, cooperativity and supercooperativity of oxygen binding by hemoglobins. *J. Exp. Biol.* 201, 1073–1084.
- (17) White, S. L. (1975) The molecular dissociation of ferrihemoglobin derivatives. *J. Biol. Chem.* 250, 1263–1268.
- (18) Eaton, W. A., Henry, E. R., Hofrichter, J., and Mozzarelli, A. (1999) Is cooperative oxygen binding by hemoglobin really understood. *Nat. Struct. Biol.* 6, 351–358.
- (19) Ishimori, K., and Morishima, I. (1988) Study of the specific heme orientation in reconstituted hemoglobins. *Biochemistry* 27, 4747–4753.
- (20) Krishna Kumar, K., Dickson, C. F., Weiss, M. J., Mackay, J. P., and Gell, D. A. (2010) AHSP ( $\alpha$ -haemoglobin-stabilizing protein) stabilizes apo- $\alpha$ -haemoglobin in a partially folded state. *Biochem. J.* 432, 275–282.
- (21) Shaeffer, J. R., McDonald, M. J., and Bunn, H. F. (1981) Assembly of normal and abnormal human hemoglobins. *Trends Biochem. Sci.* 6, 158–161.
- (22) Yip, Y. K., Waks, M., and Beychok, S. (1972) Influence of prosthetic groups on protein folding and subunit assembly. 1. Conformational differences between separated human  $\alpha$ -globins and  $\beta$ -globins. *J. Biol. Chem.* 247, 7237–7244.
- (23) McDonald, M. J., Turci, S. M., Mrabet, N. T., Himelstein, B. P., and Bunn, H. F. (1987) The Kinetics of Assembly of Normal and Variant Human Oxyhemoglobins. *J. Biol. Chem.* 262, 5951–5956.
- (24) Adachi, K., Zhao, Y., and Surrey, S. (2003) Effects of heme addition on formation of stable human globin chains and hemoglobin subunit assembly in a cell-free system. *Arch. Biochem. Biophys.* 413, 99–106.
- (25) McGovern, P., Reisberg, P., and Olson, J. S. (1976) Aggregation of Deoxyhemoglobin Subunits. *J. Biol. Chem.* 251, 7871–7879.
- (26) Kawamura, Y., Hasumi, H., and Nakamura, S. (1982) Kinetic Studies on the Reconstitution of Deoxyhemoglobin from Isolated  $\alpha$  and  $\beta$  Chains. *J. Biochem.* 92, 1227–1233.
- (27) Vasudevan, G., and McDonald, M. J. (2002) Ordered heme binding ensures the assembly of fully functional hemoglobin: A hypothesis. *Curr. Protein Pept. Sci.* 3, 461–466.
- (28) Griffith, W. P., and Kaltashov, I. A. (2003) Highly asymmetric interactions between globin chains during hemoglobin assembly revealed by electrospray ionization mass spectrometry. *Biochemistry* 42, 10024–10033.
- (29) Feng, L., Gell, D. A., Zhou, S., Gu, L., Kong, Y., Li, J., Hu, M., Yan, N., Lee, C., Rich, A. M., Armstrong, R. S., Lay, P. A., Gow, A. J., Weiss, M. J., Mackay, J. P., and Shi, Y. (2004) Molecular Mechanism of AHSP-Mediated Stabilization of  $\alpha$ -Hemoglobin. *Cell* 119, 629–640.
- (30) Loo, J. A. (2000) Electrospray Ionization Mass Spectrometry: A Technology for Studying Noncovalent Macromolecular Complexes. *Int. J. Mass Spectrom.* 200, 175–186.
- (31) Heck, A. J. R. (2008) Native mass spectrometry: A bridge between interactomics and structural biology. *Nat. Methods* 5, 927–933.
- (32) Morgner, N., and Robinson, C. V. (2012) Linking structural change with functional regulation: Insights from mass spectrometry. *Curr. Opin. Struct. Biol.* 22, 44–51.
- (33) Wang, W., Kitova, E. N., and Klassen, J. S. (2003) Influence of solution and gas phase processes on protein-carbohydrate binding affinities determined by nanoelectrospray Fourier transform ion cyclotron resonance mass spectrometry. *Anal. Chem.* 75, 4945–4955.
- (34) Liu, J., and Konermann, L. (2011) Protein-Protein Binding Affinities In Solution Determined by Electrospray Mass Spectrometry. *J. Am. Soc. Mass Spectrom.* 22, 408–417.
- (35) Cubrilovic, D., Biela, A., Sielaff, F., Steinmetzer, T., Klebe, G., and Zenobi, R. (2012) Quantifying Protein-Ligand Binding Constants using Electrospray Ionization Mass Spectrometry: A Systematic Binding Affinity Study of a Series of Hydrophobically Modified Trypsin Inhibitors. *J. Am. Soc. Mass Spectrom.* 23, 1768–1777.
- (36) Konermann, L., Ahadi, E., Rodriguez, A. D., and Vahidi, S. (2013) Unraveling the Mechanism of Electrospray Ionization. *Anal. Chem.* 85, 2–9.
- (37) Chowdhury, S. K., Katta, V., and Chait, B. T. (1990) Probing Conformational Changes in Proteins by Mass Spectrometry. *J. Am. Chem. Soc.* 112, 9012–9013.
- (38) Testa, L., Brocca, S., and Grandori, R. (2011) Charge-Surface Correlation in Electrospray Ionization of Folded and Unfolded Proteins. *Anal. Chem.* 83, 6459–6463.
- (39) Kaltashov, I. A., and Abzalimov, R. R. (2008) Do Ionic Charges in ESI MS Provide Useful Information on Macromolecular Structure? *J. Am. Soc. Mass Spectrom.* 19, 1239–1246.
- (40) Borys, A. J. H., Radford, S. E., and Ashcroft, A. E. (2004) Copopulated Conformational Ensembles of b2-Microglobulin Uncovered Quantitatively by Electrospray Ionization Mass Spectrometry. *J. Biol. Chem.* 279, 27069–27077.
- (41) Kim, M.-Y., Maier, C. S., Reed, D. J., and Deinzer, M. L. (2002) Conformational changes in chemically modified *Escherichia coli* thioredoxin monitored by H/D exchange and electrospray mass spectrometry. *Protein Sci.* 11, 1320–1329.
- (42) Vis, H., Heinemann, U., Dobson, C. M., and Robinson, C. V. (1998) Detection of a Monomeric Intermediate Associated with Dimerization of Protein Hu by Mass Spectrometry. *J. Am. Chem. Soc.* 120, 6427–6428.
- (43) Fändrich, M., Tito, M. A., Leroux, M. R., Rostom, A. A., Hartl, F. U., Dobson, C. M., and Robinson, C. V. (2000) Observation of the noncovalent assembly and disassembly pathways of the chaperone complex MtGimC by mass spectrometry. *Proc. Natl. Acad. Sci. U.S.A.* 97, 14151–14155.

- (44) Sharon, M., Witt, S., Glasmacher, E., Baumeister, W., and Robinson, C. V. (2007) Mass spectrometry reveals the missing links in the assembly pathway of the bacterial 20 S proteasome. *J. Biol. Chem.* 282, 18448–18457.
- (45) Boys, B. L., and Konermann, L. (2007) Folding and Assembly of Hemoglobin Monitored by Electrospray Mass Spectrometry Using an On-line Dialysis System. *J. Am. Soc. Mass Spectrom.* 18, 8–16.
- (46) Smith, A. M., Jahn, T. R., Ashcroft, A. E., and Radford, S. E. (2006) Direct Observation of Oligomeric Species formed in the Early Stages of Amyloid Formation using Electrospray Ionization Mass Spectrometry. *J. Mol. Biol.* 364, 9–19.
- (47) Kang, Y., Terrier, P., and Douglas, D. J. (2011) Mass Spectra and Ion Collision Cross Sections of Hemoglobin. *J. Am. Soc. Mass Spectrom.* 22, 290–299.
- (48) Scarff, C. A., Patel, V. J., Thalassinou, K., and Scrivens, J. H. (2009) Probing Hemoglobin Structure by Means of Traveling-Wave Ion Mobility Mass Spectrometry. *J. Am. Soc. Mass Spectrom.* 20, 625–631.
- (49) Griffith, W. P., and Kaltashov, I. A. (2007) Protein Conformational Heterogeneity as a Binding Catalyst: ESI-MS Study of Hemoglobin H Formation. *Biochemistry* 46, 2020–2026.
- (50) Boys, B. L., Kuprowski, M. C., and Konermann, L. (2007) Symmetric Behavior of Hemoglobin  $\alpha$ - and  $\beta$ -Subunits during Acid-Induced Denaturation Observed by Electrospray Mass Spectrometry. *Biochemistry* 46, 10675–10684.
- (51) Adams, P. A. (1977) The Kinetics of the Recombination Reaction between Apomyoglobin and Alkaline Haematin. *Biochem. J.* 163, 153–158.
- (52) He, F., Hendricksen, C. L., and Marshall, A. G. (2000) Unequivocal Determination of Metal Atom Oxidation State in Naked Heme Proteins: Fe(III)Myoglobin, Fe(III)Cytochrome c, Fe(III)-Cytochrome b5, and Fe(III) Cytochrome b5 L47R. *J. Am. Soc. Mass Spectrom.* 11, 120–126.
- (53) Crosby, W. H., and Houchin, D. N. (1957) Preparing Standard Solutions of Cyanmethemoglobin. *Blood* 12, 1132–1136.
- (54) Crespin, M. O., Boys, B. L., and Konermann, L. (2005) The reconstitution of unfolded myoglobin with hemin dicyanide is not accelerated by fly casting. *FEBS Lett.* 579, 271–274.
- (55) Yee, S., and Peyton, D. H. (1991) Proton NMR investigation of the reconstitution of equine myoglobin with hemin dicyanide. *FEBS Lett.* 290, 119–122.
- (56) Xu, G., and Chance, M. R. (2007) Hydroxyl Radical-Mediated Modification of Proteins as Probes for Structural Proteomics. *Chem. Rev.* 107, 3514–3543.
- (57) Sage, J. T., Morikis, D., and Champion, P. M. (1991) Spectroscopic Studies of Myoglobin at Low pH: Heme Structure and Ligation. *Biochemistry* 30, 1227–1237.
- (58) Wittung-Stafshede, P., Gray, H. B., and Winkler, J. R. (1997) Rapid Formation of a Four-Helix Bundle. Cytochrome b562 Folding Triggered by Electron Transfer. *J. Am. Chem. Soc.* 119, 9562–9563.
- (59) Bobst, C. E., Wang, S. H., Shen, W. C., and Kaltashov, I. A. (2012) Mass spectrometry study of a transferrin-based protein drug reveals the key role of protein aggregation for successful oral delivery. *Proc. Natl. Acad. Sci. U.S.A.* 109, 13544–13548.
- (60) Benjwal, S., Verma, S., Röhm, K.-H., and Gursky, O. (2006) Monitoring protein aggregation during thermal unfolding in circular dichroism experiments. *Protein Sci.* 15, 635–639.
- (61) Verkerk, U. H., and Kebarle, P. (2005) Ion-Ion and Ion-Molecule Reactions at the Surface of Proteins Produced by Nanospray. Information on the Number of Acidic Residues and Control of the Number of Ionized Acidic and Basic Residues. *J. Am. Soc. Mass Spectrom.* 16, 1325–1341.
- (62) Simmons, D. A., Dunn, S. D., and Konermann, L. (2003) Conformational Dynamics of Partially Denatured Myoglobin Studied by Time-Resolved Electrospray Mass Spectrometry With Online Hydrogen-Deuterium Exchange. *Biochemistry* 42, 5896–5905.
- (63) Dobson, C. M. (2003) Protein folding and misfolding. *Nature* 426, 884–890.
- (64) Leutzing, Y., and Beychok, S. (1981) Kinetics and mechanism of heme-induced refolding of human  $\alpha$ -globin. *Proc. Natl. Acad. Sci. U.S.A.* 78, 780–784.
- (65) Adams, P. A., and Berman, M. C. (1980) Kinetics and Mechanism of the Interaction between Human-Serum Albumin and Monomeric Hemin. *Biochem. J.* 191, 95–102.
- (66) Robinson, C. R., Liu, Y., Thomson, J. A., Sturtevant, J. M., and Sligar, S. G. (1997) Energetics of Heme Binding to Native and Denatured States of Cytochrome b<sub>562</sub>. *Biochemistry* 36, 16141–16146.
- (67) Collings, B. A., and Douglas, D. J. (1996) Conformation of Gas-Phase Myoglobin Ions. *J. Am. Chem. Soc.* 118, 4488–4489.
- (68) Kuzelova, K., Mrhalova, M., and Hrkál, Z. (1997) Kinetics of heme interaction with heme-binding proteins: The effect of heme aggregation state. *Biochim. Biophys. Acta* 1336, 497–501.
- (69) Uetrecht, C., Barbu, I. M., Shoemaker, G. K., van Duijn, E., and Heck, A. J. R. (2011) Interrogating viral capsid assembly with ion mobility–mass spectrometry. *Nat. Chem.* 3, 126–132.